

OPEN ACCESS

Experimental Confirmation of C-Rate Dependent Minima Shifts in Arrhenius Plots of Li-Ion Battery Aging

To cite this article: Maral Bozorgchenani *et al* 2022 *J. Electrochem. Soc.* **169** 030509

View the [article online](#) for updates and enhancements.



ECS Membership = Connection

ECS membership connects you to the electrochemical community:

- Facilitate your research and discovery through ECS meetings which convene scientists from around the world;
- Access professional support through your lifetime career;
- Open up mentorship opportunities across the stages of your career;
- Build relationships that nurture partnership, teamwork—and success!

Join ECS!

Visit electrochem.org/join





Experimental Confirmation of C-Rate Dependent Minima Shifts in Arrhenius Plots of Li-Ion Battery Aging

Maral Bozorgchenani,^{1,=} Gints Kucinskis,^{1,2,=} Margret Wohlfahrt-Mehrens,^{1,*} and Thomas Waldmann^{1,z}

¹ZSW—Zentrum für Sonnenenergie- und Wasserstoff-Forschung, Baden-Württemberg, D-89081 Ulm, Germany

²Institute of Solid State Physics, University of Latvia, Riga LV-1063, Latvia

Li-ion batteries show a minimum of their aging rate at a certain temperature. This minimum in the corresponding Arrhenius plot expresses the longest cycle life at a certain C-rate. By characterizing aging of laboratory-made pouch cells and commercial 21700 cells as a function of C-rate and ambient temperature, we confirm that this minimum indeed shifts with the charging C-rate. Increasing C-rates lead to higher optimal ambient temperatures with respect to the aging rate. The differences between both cell types are discussed regarding the specific energy and anode coating thickness of the tested cells.

© 2022 The Author(s). Published on behalf of The Electrochemical Society by IOP Publishing Limited. This is an open access article distributed under the terms of the Creative Commons Attribution 4.0 License (<http://creativecommons.org/licenses/by/4.0/>), which permits unrestricted reuse of the work in any medium, provided the original work is properly cited. [DOI: 10.1149/1945-7111/ac580d]



Manuscript submitted November 19, 2021; revised manuscript received January 18, 2022. Published March 4, 2022.

The lifetime of Li-ion batteries is a critical issue, especially for applications such as electric cars or stationary energy storage. Therefore, low aging rates are favorable. Aging mechanisms are unwanted side reactions and increase the aging rate in different ways. For instance, the aging mechanism of continuing solid electrolyte interphase (SEI) growth is known to increase the aging rate with increasing temperature.^{1–3} Liaw et al.⁴ showed that the capacity fade in the high temperature regime (+25 °C to +65 °C) follows an Arrhenius-like behavior. This is not surprising, since the Arrhenius equation

$$r = A \exp\left(-\frac{E_a}{k_B T}\right) \quad [1]$$

is well known to describe the increase of the rate r for many chemical reactions.⁵ In this equation, A is the pre-exponential factor, E_a the activation energy, k_B the Boltzmann constant, and T the absolute temperature.

Observing cycling aging in a wider temperature range (–20 °C to +70 °C), we had observed for commercial 18650-type Li-ion cells that the slope in the Arrhenius plot changes.² This slope change indicates a change of the main aging mechanism.⁵ In case of Li-ion batteries, this temperature dependent change of the main aging mechanism usually involves Li plating in the low temperature range.^{2,3,6–8}

The coincidence of both main aging mechanisms happens at a certain temperature, where the aging rates show a minimum in the Arrhenius plot. Yang et al.³ showed by simulations that this minimum shifts to higher temperatures if the charging C-rate is increased.

In this communication, we investigated this shift of the minimum of the aging rate experimentally by cycling aging of pouch cells made in laboratory as well as commercial 21700 cells.

Experimental

Pouch cells (~0.1 Ah) were built on lab scale using double side coated graphite anodes (2.5 mAh cm⁻²), single side coated NMC111 cathodes (2.06 mAh cm⁻²), and Celgard 2325 separator. The electrodes were vacuum dried at 130 °C for 9 h. The pouch cells were assembled in the dry room (dew point < –62 °C). After cell assembly, the pouch cells were dried in the antechamber of the glove box (Mbraun, O₂ and H₂O < 0.3 ppm) at 80 °C for 16 h. The cells were filled inside an Ar glove box with 900 μl 1.0 M LiPF₆ in EC:EMC (3:7 wt) + 2% VC electrolyte.

All electrochemical tests were performed using Basytec CTS and Maccor 4200 systems in climate chambers (Vötsch, CTS) or at room temperature (23 ± 3 °C). Formation was carried out after a rest of 12 h following three cycles with 0.1C (2.7 V to 4.2 V) by a constant-current/constant-voltage protocol (CC/CV, CV until 0.05C). The cells were mechanically pressed using a cell holder, resulting in ~100 N perpendicular to the stack uniformly distributed on the cell surface. For 0.2C at least two cells were tested for the each condition. However, for 0.5C and 1C only in some cases two of more cells were tested.

Cycling aging of the lab-made pouch cells at ambient temperatures in the range of –15 °C to +60 °C were performed at rates of 0.2C, 0.5C, and 1C (CC-CV, CV until 0.02C).

50 commercial cells of the same type were initially tested regarding resistance (Hioki RM3548 @1 kHz, 12.9 ± 0.3 mΩ), mass (69.5 ± 0.1 g), and voltage (3.679 ± 0.002 V). The low standard deviations showed that the cells are usable for further tests. We performed cycling aging of the commercial 21700 cells at ambient temperatures in the range of –15 to +55 °C at charge rates of 0.2C, 0.4C, and 0.6C (CC-CV, CV until 0.05C) and discharge rate of 0.5C (CC). For each C-rate at certain ambient temperature two cells were tested except for 55 °C, where only one cell was tested.

Results and Discussion

Figure 1 shows the capacity fade for lab-made pouch cells at rates of 0.2C, 0.5C, and 1C. For 0.2C (Fig. 1a), the curves for all temperatures from –10 °C to +45 °C have the same curve shape, however, the aging rates are different. The aging rates increase by increasing (red arrow) or decreasing (blue arrow) the temperature from +5 °C to +45 °C or to –10 °C, respectively. The slowest aging rate for the lab-made pouch cells is observed at +5 °C for 0.2C.

For 0.5C (Fig. 1b), the aging of the pouch cells is slowest at +15 °C which is 10 °C higher than the slowest aging temperature for 0.2C. We observe two trends of growing aging rate with increasing temperature to +50 °C (red arrow) and decreasing the temperature to –15 °C (blue arrow).

By increasing the C-rate to 1C (Fig. 1c), we observe that the aging rate is slowest at ~35 °C for the pouch cells. Both, by increasing the temperature to +60 °C (red arrow) and decreasing the temperature to –10 °C (blue arrow), aging becomes faster. Stronger Li plating can be expected for –5 °C and –10 °C where the SOH decreases to 88% in less than 50 cycles.

The optimum temperature depends on the anode characteristics.³ In our previous experiments, performed on 18650 type high-power cells at 1C, the aging was slowest at 25 °C² while for the lab-made pouch cells in this study, the optimum temperature was ~35 °C.

⁼These authors contributed equally to this work.

*Electrochemical Society Member.

^zE-mail: thomas.waldmann@zsw-bw.de

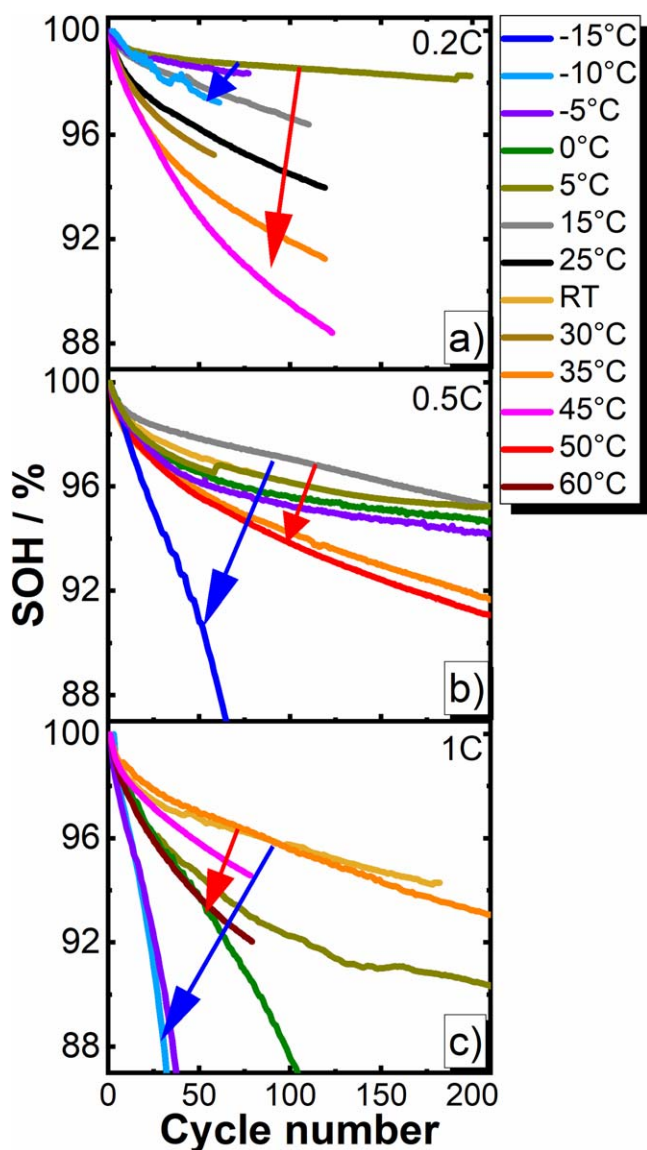


Figure 1. Capacity fade curves of lab-made pouch cells at different temperatures and C-rates; (a) 0.2C; (b) 0.5C; (c) 1C. The arrows show trends of increasing aging rates.

Figure 2 shows the capacity fade curves of commercial 21700 cells at rates of 0.2C, 0.4C, and 0.6C in the temperature range from $-10\text{ }^{\circ}\text{C}$ to $+55\text{ }^{\circ}\text{C}$. For 0.2C (Figure 2a), aging gets faster by increasing the temperature from $+15\text{ }^{\circ}\text{C}$ to $+45\text{ }^{\circ}\text{C}$ and decreasing temperature from $+15\text{ }^{\circ}\text{C}$ to $-10\text{ }^{\circ}\text{C}$. For the lab-made pouch cells (Fig. 1a), the capacity fade at low temperatures was much slower under the same cycling conditions.

For the 21700 cells cycled at 0.4C and 0.6C, the trends are similar as for 0.2C, however, the lowest aging rates are observed at higher temperatures. These trends can be better analyzed in the Arrhenius plots in Fig. 3. The Arrhenius plots were calculated from the aging rates for the first 40 cycles for the lab-made pouch cells and commercial 21700 cells from Figs. 1 and 2. We note that the aging rate was calculated in decrease of SOH per cycle to generate comparable values for different C-rates. It is further noted that the aging rate changes with cycles for both cell types in a different way, however, evaluation of the first 40 cycles is a good compromise to allow comparability of both cell types.

The Arrhenius plots of both cell types show minima which is consistent with previous measurements in our group² and simulations by Yang et al.³ These minima shift with C-rate. For the lab-made

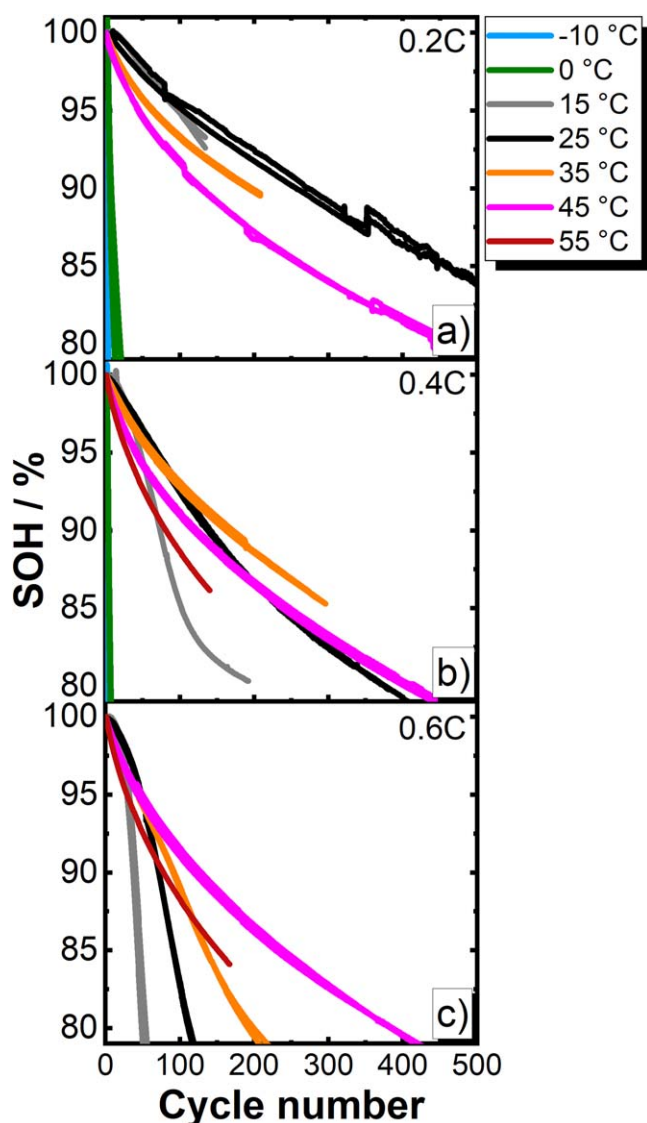


Figure 2. Capacity fade curves of commercial 21700 cells at different temperatures and C-rates. (a) 0.2C; (b) 0.4C; (c) 0.6C.

pouch cells, the minima for 0.2C, 0.5C, and 1C are at $+5\text{ }^{\circ}\text{C}$, $+15\text{ }^{\circ}\text{C}$, and $+35\text{ }^{\circ}\text{C}$, respectively. For the commercial 21700 cells, the lowest measured aging rate for 0.2C, 0.4C, and 0.6C are at $+15\text{ }^{\circ}\text{C}$, $+18\text{ }^{\circ}\text{C}$, and $+25\text{ }^{\circ}\text{C}$ respectively. This confirms the trend which was predicted in simulations by Yang et al.³ Furthermore, the fact that the minimum in the Arrhenius plot shifts to lower temperature with lower C-rate is consistent with calendar aging experiments, where no charging is involved (“0C”) with commercial 18650 cells which did not show a minimum in the Arrhenius plot in the range of $+6\text{ }^{\circ}\text{C}$ to $+60\text{ }^{\circ}\text{C}$.⁹

For the commercial 21700 cells, the minima in the Arrhenius plots are shifted to higher temperatures compared to the lab-made pouch cells. The reason is that the anode of the commercial cells have a single side coated thickness of $93 \pm 4\text{ }\mu\text{m}$ (estimation using 262 Wh kg^{-1} and Eq. 1 from Ref. 10) while the lab-made pouch cells have an anode thickness of only $58\text{ }\mu\text{m}$. As it is shown by Yang et al.,³ increase of anode thickness leads to an earlier onset of Li plating. Additional influences are likely to originate from differences of porosity and tortuosity, however, this is outside of the scope of this communication.

Burns et al.⁶ studied aging of 0.22 Ah pouch cells with a single side anode coating thickness of $51\text{ }\mu\text{m}$ with C-rates ranging from C/50 to 3C in two different ambient temperatures. They observed by Post-Mortem analysis that for $+12\text{ }^{\circ}\text{C}$, Li plating starts at $\sim 0.5\text{C}$ while for $+50\text{ }^{\circ}\text{C}$ it starts from $\sim 2\text{C}$. The anode thickness is in the

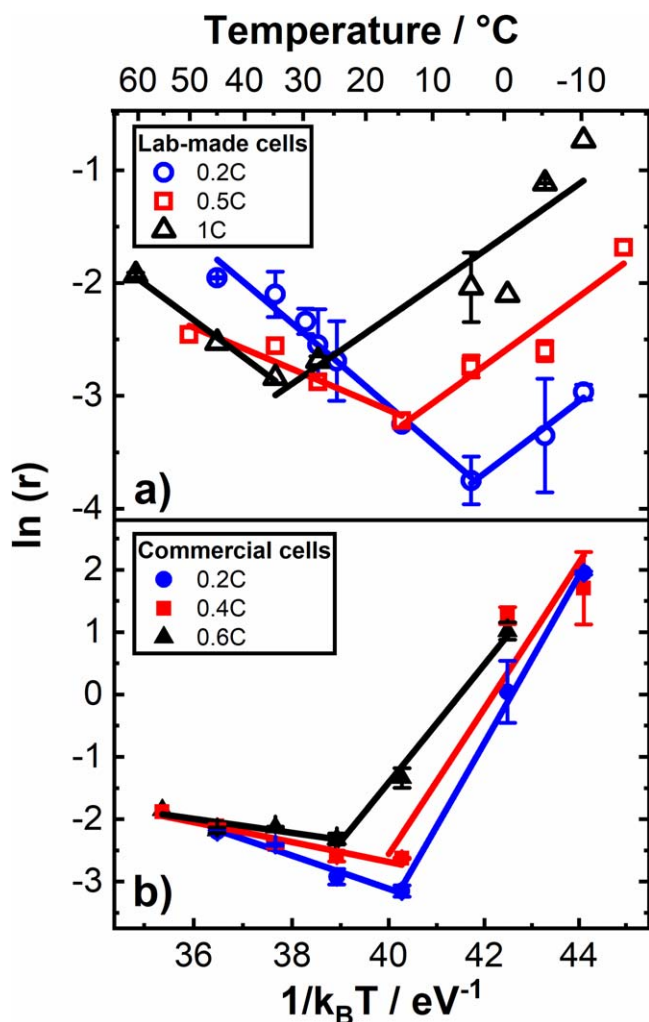


Figure 3. Arrhenius plots constructed from capacity fade (cycles 1 to 40) for (a) lab-made pouch cells and (b) commercial 21700 cells at different C-rates.

range of our lab-made pouch cells and onset of Li plating at 0.5C was around +12 °C in their case⁶ and +15 °C in the present study.

In large cells, gradients of temperature¹¹ and current density¹² evolve due to current flow. The results from the present study suggest that these gradients could lead to different aging mechanisms inside such cells, especially at high charging C-rates.

Conclusions

For cycling aging, Li-ion cells show an optimum temperature at which the aging rate is lowest. This optimum arises from a transition

between two competing aging mechanisms, most likely SEI growth dominating at high temperatures and Li plating at low temperatures.

We observed experimentally, that the temperature at which the aging rate of the cell is lowest increases with higher C-rates. This trend was observed for both lab-made pouch cells and commercial 21700 cells, and is consistent with simulations by Yang et al.³

By testing two different cell types we demonstrate experimentally that the crossover temperature depends on the electrode thickness, i.e. high-energy cells show the mechanism change to Li deposition at higher temperatures. Considering the shift of the dominant aging mechanism as a function of temperature and charging C-rate can help to design battery systems with extended service life. In large cells, gradients of temperature and current density could lead to different aging mechanisms inside a single cell. Further work into this direction is ongoing in our labs.

Acknowledgments

The part of the research performed at ZSW was carried out in the framework of the industrial collective research program (IGF no. 20884 N/2). It was supported by the Federal Ministry for Economic Affairs and Climate Action (BMWK) through the AiF (German Federation of Industrial Research Associations eV) based on a decision taken by the German Bundestag. G.K. acknowledges funding from the Latvian Council of Science (lzp-2020/1-0425) and from the European Union's Horizon 2020 Framework Program under grant agreement No. 739508, project CAMART2.

ORCID

Maral Bozorgchenani <https://orcid.org/0000-0001-9395-1283>
 Gints Kucinskis <https://orcid.org/0000-0001-9432-2358>
 Margret Wohlfahrt-Mehrens <https://orcid.org/0000-0002-5118-5215>
 Thomas Waldmann <https://orcid.org/0000-0003-3761-1668>

References

1. M. Broussely, S. Herreyre, P. Biensan, P. Kaszlejna, K. Nechev, and R. J. Staniewicz, *J. Power Sources*, **97–98**, 13 (2001).
2. T. Waldmann, M. Wilka, M. Kasper, M. Fleischhammer, and M. Wohlfahrt-Mehrens, *J. Power Sources*, **262**, 129 (2014).
3. X.-G. Yang and C.-Y. Wang, *J. Power Sources*, **402**, 489 (2018).
4. B. Y. Liaw, E. P. Roth, R. G. Jungst, G. Nagasubramanian, H. L. Case, and D. H. Dougherty, *J. Power Sources*, **119–121**, 874 (2003).
5. P. W. Atkins, *Physical Chemistry* (Oxford University Press, Oxford) (1990).
6. J. C. Burns, D. A. Stevens, and J. R. Dahn, *J. Electrochem. Soc.*, **162**, A959 (2015).
7. T. Waldmann, B.-I. Hogg, M. Kasper, S. Grolleau, C. G. Couceiro, K. Trad, B. P. Matadi, and M. Wohlfahrt-Mehrens, *J. Electrochem. Soc.*, **163**, A1232 (2016).
8. T. Waldmann, B.-I. Hogg, and M. Wohlfahrt-Mehrens, *J. Power Sources*, **384**, 107 (2018).
9. T. Waldmann, M. Kasper, and M. Wohlfahrt-Mehrens, *Electrochim. Acta*, **178**, 525 (2015).
10. J. B. Quinn, T. Waldmann, K. Richter, M. Kasper, and M. Wohlfahrt-Mehrens, *J. Electrochem. Soc.*, **165**, A3284 (2018).
11. T. Grandjean, A. Barai, E. Hosseinzadeh, Y. Guo, A. McGordon, and J. Marco, *J. Power Sources*, **359**, 215 (2017).
12. S. V. Erhard et al., *J. Electrochem. Soc.*, **164**, A6324 (2017).